Model-Independent Formation Tracking of Multiple Euler–Lagrange Systems via Bounded Inputs

Leimin Wang, *Member, IEEE*, Haibo He, *Fellow, IEEE*, Zhigang Zeng, *Senior Member, IEEE*, and Ming-Feng Ge, *Member, IEEE*

***Abstract*—This article addresses two kinds of formation tracking problems, namely: 1) the practical formation tracking (PFT) problem and 2) the zero-error formation tracking (ZEFT) problem for multiple Euler–Lagrange systems with input disturbances and unknown models. In these problems, the bounded input constraint, which can be possibly caused by actuator saturation and power limitations, is taken into consideration. Then, the two classes of model-independent distributed control approaches, in which the prior information (i.e., the structures and features) of the system model is not used, are proposed correspondingly. Based on the nonsmooth analysis and Lyapunov stability theory, several novel criteria for achieving PFT and ZEFT of multiple Euler–Lagrange systems are derived. Finally, numerical simulations and comparisons are presented to verify the validity and effectiveness of the proposed control approaches.**

***Index Terms*—Actuator saturation, formation tracking, input disturbance, multiple Euler–Lagrange systems.**

I. Introduction

The FORMATION tracking problem, as a critical topic in cooperative control of multiagent systems, has shown significant value and drawn increasing attention in past decades due to its widespread applications in unmanned vehicles [1]–[5], networked systems [6]–[10], and robotic teams [11]–[14]. Besides, the distributed control approach has been widely adopted in dealing with the formation tracking problems [15]–[21], due to its lower communication cost compared with the centralized one. For instance, Zuo *et al.* [15] proposed the distributed control approach to realize the output formation tracking of the heterogeneous linear multiagent systems. In [16], the distributed time-varying formation tracking problem was addressed for second-order multiagent systems with switching topology. Then, the distributed sliding-mode control was designed for the finite-time formation tracking in [17]. Moreover, Yu *et al.* [18], [19] extended the formation tracking control problem to nonlinear multiagent systems and obtained several practical formation tracking (PFT) results. In [20], the formation robust tracking problem was studied for multiagent systems with parameter uncertainties and external disturbances. Chen and Ren [21] discussed the inherent connection between the dynamic region-following formation control and distributed average tracking, and they also made an attempt on the applications of distributed average tracking algorithms to achieve distributed control.

On the other hand, increasing research attention has focused on the multiagent systems whose dynamic behaviors are described as nonlinear dynamics [22], [23], specifically, the Euler–Lagrange systems [24]–[27]. Such nonlinear Euler–Lagrange systems can be used to represent a broad class of engineering systems, including autonomous vehicles [28]; aerospace systems [29], [30]; and mobile robots [31]–[33], due to their unique dynamic characteristics. It thus leads to the generation of some recent research that concentrates on multiple Euler–Lagrange systems employing the distributed control approaches [34]–[38]. Especially, it is of great importance and significance to consider multiple Euler–Lagrange systems instead of the traditional linear or nonlinear multiagent systems in dealing with the formation tracking problems [39].

It is worth mentioning that the distributed control approaches in [40]–[44] are designed based on the system models with normal or estimated dynamic parameters, that is, the prior structures and features of the system models are required. In this manner, the designed control approaches are called model-based control [45]. However, such model-based control cannot be constructed and established, in the case that the model information, that can be directly employed in control design, is limited [46], [47]. Then, the model-independent control approach has been a better choice compared with the model-based one in such a case [48], [49]. Therefore, designing model-independent control for solving the coordination problems has become a popular topic recently. For instance, our previous work [50] designed some model-independent

Manuscript received February 14, 2019; revised June 11, 2019 and August 16, 2019; accepted August 22, 2019. Date of publication October 31, 2019; date of current version April 15, 2021. This work was supported in part by the National Natural Science Foundation of China under Grant 61703377, in part by the State Scholarship Fund of China Scholarship Council under Grant 201806415020, and in part by the National Science Foundation under Grant ECCS 1917275. This article was recommended by Associate Editor Z.-G. Hou. *(Corresponding author: Haibo He.)*

L. Wang is with the School of Automation, China University of Geosciences, Wuhan 430074, China, and also with the Hubei Key Laboratory of Advanced Control and Intelligent Automation for Complex Systems, China University of Geosciences, Wuhan 430074, China (e-mail: wangleimin@cug.edu.cn).

H. He is with the Department of Electrical, Computer, and Biomedical Engineering, University of Rhode Island, Kingston, RI 02881 USA (e-mail: he@ele.uri.edu).

Z. Zeng is with the School of Artificial Intelligence and Automation, Huazhong University of Science and Technology, Wuhan 430074, China (e-mail: zgzeng@hust.edu.cn).

M.-F. Ge is with the School of Mechanical Engineering and Electronic Information, China University of Geosciences, Wuhan 430074, China (e-mail: fmgabc@163.com).

Color versions of one or more figures in this article are available at https://doi.org/10.1109/TCYB.2019.2938398.

Digital Object Identifier 10.1109/TCYB.2019.2938398

2168-2267 © 2019 IEEE. Personal use is permitted, but republication/redistribution requires IEEE permission.
See https://www.ieee.org/publications/rights/index.html for more information.

Authorized licensed use limited to: IEEE Editors-in-Chief. Downloaded on June 14,2021 at 19:52:24 UTC from IEEE Xplore. Restrictions apply.

distributed proportional–derivative-like control approaches to deal with the target tracking problem of the networked Euler–Lagrange systems without using model information. However, only practical stability can be achieved for the considered closed-loop system, which thus motivates the study on the zero-error tracking problem of multiple Euler–Lagrange systems in this article.

In addition to considering the model-independent control approach, another important topic in the control area is to develop control algorithms with bounded input. That is mainly due to the inevitable actuator saturation and power limitations in engineering applications [51]. Besides, designing control algorithms with bounded inputs for stabilizing multiple Euler–Lagrange systems has become extraordinarily difficult, on account of the fact that there are generally a large number of agents in their applications [52]. In light of such a critical impact of the bounded input (i.e., input saturation) constraints, great efforts have been made to the cooperative tracking problem subjected to such constraints [53]–[57]. However, the control algorithms presented in [52]–[56] can only drive the systems to reach PFT. More important, the input disturbances, which are inevitable in practical applications, have not been taken into consideration in the aforementioned literature [51]–[57]. Thus, developing control approaches for multiple Euler–Lagrange systems under input disturbances and bounded input constraints, to solve both the PFT problem and zero-error formation tracking (ZEFT) problem under a uniform framework, are still unaccomplished.

Motivated by the above discussions, this article proposes two kinds of model-independent control approaches with the consideration of input disturbances and bounded input constraints to overcome the challenging problems of both the PFT and ZEFT for multiple Euler–Lagrange systems. The main contributions are three-fold.

1) Different from the model-based control approaches investigated in [40]–[44] that require prior information of structures and features of the system models, the presented distributed control approaches are model independent, which can be employed to deal with the control systems with limited model information and provide theoretical guidance for such problems.
2) In [16], [18]–[20], [39], and [49], the formation tracking problem was addressed without considering the input disturbances and bounded input constraints. Since these constraints are inevitable in some practical applications, it is of great significance to study the formation tracking problem with such constraints. Thus, in this article, the formation tracking problem of multiple Euler–Lagrange systems with such constraints is successfully solved by using the presented model-independent control.
3) Compared with the study in [18], [19], and [50] where only the PFT problem was solved under distributed control, we present a uniform framework for solving both the PFT problem and ZEFT problem for multiple Euler–Lagrange systems.

Notation: $\mathcal{R}$, $\mathcal{R}_+$, $\mathcal{R}^n$, and $\mathcal{R}^{n\times n}$ denote the set of real numbers, positive real numbers, the $n \times 1$ real column vector, and $n \times n$ real matrix, respectively. $\mathbf{1}_n = \mathrm{col}(1, 1, \dots, 1) \in \mathcal{R}^n$ is the identity vector and I_n is the $n \times n$ identity matrix. $\mathrm{sign}(\cdot)$ is the signum function. For a vector $\omega = \mathrm{col}(\omega_1, \omega_2, \dots, \omega_n) \in \mathcal{R}^n$, $\|\omega\| = (\sum_{i=1}^n |\omega_i|^2)^{1/2}$ denotes the Euclidean norm and $\|\omega\|_1 = \sum_{i=1}^n |\omega_i|$, $\|\omega\|_\infty = \max_i |\omega_i|$. For a matrix $C \in \mathcal{R}^{n\times n}$, the norm $\|C\| = \sqrt{\lambda_{\max}(C^T C)}$, where $\lambda_{\max}(\cdot)$ denotes the maximum eigenvalue. $\tanh(\cdot)$, $\mathrm{sech}(\cdot)$, and $\cosh(\cdot)$ denote the hyperbolic tangent, secant, and cosine functions, respectively, and $\tanh(\omega) = \mathrm{col}(\tanh(\omega_1), \dots, \tanh(\omega_n))$, $\cosh(\omega) = \mathrm{col}(\cosh(\omega_1), \dots, \cosh(\omega_n))$. $\mathrm{sign}(\cdot)$ denotes the standard signum function.

II. Preliminaries

A. Graph Theory

Throughout this article, we consider a weighted directed robotic network $\mathscr{G} = (\mathscr{V}, \mathscr{E}, \mathscr{A})$ with a set of N robots, a set of nodes $\mathscr{V} = \{v_1, v_2, \dots, v_N\}$, a set of directed edges $\mathscr{E} = \{(v_i, v_j) : v_i, v_j \in \mathscr{V}\} \subseteq \mathscr{V} \times \mathscr{V}$, and a weighted adjacency matrix $\mathscr{A} = [a_{ij}] \in \mathcal{R}^{N\times N}$. A directed edge $\mathscr{E}_{ij}$ in the robotic network is denoted by the ordered pair of robots (v_i, v_j), where v_i and v_j are called the terminal and initial robots, respectively, which means that robot v_i can receive information from robot v_j. If there is a directed edge $(v_i, v_j) \in \mathscr{E}$, then $a_{ij} > 0$; otherwise, $a_{ij} = 0$. Besides, self-loop is not allowed, that is, $a_{ii} = 0$. The target of the directed robotic network is denoted by robot 0 and the interaction between the robots and target is represented by a matrix $B = \mathrm{diag}\{a_{10}, a_{20}, \dots, a_{N0}\}$, $\mathcal{N}_i = \{j \in \mathbb{N} : (v_i, v_j) \in \mathscr{E}, j \neq i\}$ is a set of neighbors of robot i, and $\mathbb{N} = \{0, 1, 2, \dots, N\}$. $\Gamma = \{\zeta_1, \dots, \zeta_N\}$ denotes a set of formation patterns at time t, where ζ_i is the desired position of robot v_i. $L = [l_{ij}] \in \mathcal{R}^{N\times N}$ is the Laplacian matrix of the graph and it is defined by $L = \mathrm{diag}(A\mathbf{1}_N) - A$, that is, $l_{ii} = \sum_{j=1, j\neq i}^N a_{ij}$, $l_{ij} = -a_{ij}$, $i \neq j$. For a connected graph, the Laplacian matrix L has a simple zero eigenvalue with the associated eigenvector $\mathbf{1}_N L = 0$.

B. Problem Formulation

The dynamics of the ith subsystem under input disturbances are given as [58]

$$M_i(q_i)\ddot{q}_i + C_i(q_i, \dot{q}_i)\dot{q}_i + D_i\dot{q}_i + g_i(q_i) = u_i + \kappa_i \tag{1}$$

where $i \in \mathscr{N} = \{1, 2, \dots, N\}$; $t \in T = [t_0, \infty)$; $t_0 \geq 0$ is the initial time; and $q_i(t) \in \mathcal{R}^n$, $\dot{q}_i(t) \in \mathcal{R}^n$, and $\ddot{q}_i(t) \in \mathcal{R}^n$ denote the link position, velocity, and acceleration, which are simplified as q_i, $\dot{q}_i$, and $\ddot{q}_i$. $M_i(q_i)$, $C_i(q_i, \dot{q}_i) \in \mathcal{R}^{n\times n}$ denote the inertia matrix and the centrifugal–Coriolis matrix, respectively. $g_i(q_i) \in \mathcal{R}^n$ is the gravity vector. $D_i \in \mathcal{R}^{n\times n}$ represents the matrix composed of the damping friction coefficients. $\kappa_i \in \mathcal{R}^n$ denotes the input disturbance. u_i is torque control.

The time-varying moving target for the multirobot system (1) is given as $\dot{y}_0 = z_0$, $\dot{z}_0 = f(t, z_0)$, where $f : T \times \mathcal{R}^n \to \mathcal{R}^n$ is the nonlinear dynamics of the target.

Then, we present the following assumptions for system (1).

Assumption 1: The directed robotic network $\mathscr{G}$ has a directed spanning tree.

Assumption 2: The vectors $z_0, \dot{z}_0 \in \mathcal{R}^n$ are bounded, that is, there exist constants $\alpha_1, \alpha_2, \eta_1$, and $\eta_2 \in \mathcal{R}_+$ such that

$$\sup_{t\in T} \|z_0\| \leq \alpha_1, \sup_{t\in T} \|\dot{z}_0\| \leq \alpha_2$$
$$\sup_{t\in T} \|z_0\|_\infty \leq \eta_1, \sup_{t\in T} \|\dot{z}_0\|_\infty \leq \eta_2.$$

Authorized licensed use limited to: IEEE Editors-in-Chief. Downloaded on June 14,2021 at 19:52:24 UTC from IEEE Xplore. Restrictions apply.

TABLE I
CONTROL PROCESS OF THE SATURATED CONTROL INPUTS (3) AND (26)

Algorithm: Main input: Main output:	Control input (3) $y_0, z_0, \zeta_i, \beta_{1i}, \beta_{2i}, \eta_1, \eta_2, u_{i,\max}$ $q_i, \dot{q}_i$	Control input (26) $y_0, z_0, \zeta_i, \beta_{1i}, \beta_{2i}, \beta_{3i}, \eta_1, \eta_2, u_{i,\max}$ $q_i, \dot{q}_i$
Step 1	Initialization: The target is globally reachable. Let the initial values $\in L_\infty \cap L_2$ such that $q_i, \dot{q}_i \in L_\infty \cap L_2$ as $t \in [t_0, t^*]$.	Initialization: The target is globally reachable. Let the initial values $\in L_\infty \cap L_2$ such that $q_i, \dot{q}_i \in L_\infty \cap L_2$ as $t \in [t_0, t^*]$.
Step 2	Design the bounded control input (3), the nonsmooth estimators (4) and (5). Choose $\eta_1 > \sup_{t\in T} \|z_0\|_\infty, \eta_2 > \sup_{t\in T} \|\dot{z}_0\|_\infty$ such that $y_i \equiv y_0 + \zeta_i, z_i \equiv z_0$ for $t \geq t^*$.	Design another bounded control input (26), the nonsmooth estimators (4) and (5). Choose $\eta_1 > \sup_{t\in T} \|z_0\|_\infty, \eta_2 > \sup_{t\in T} \|\dot{z}_0\|_\infty$ such that $y_i \equiv y_0 + \zeta_i, z_i \equiv z_0$ for $t \geq t^*$.
Step 3	Combine with (3)-(5) into (1), system (16) is obtained. Choose proper β_{1i}, β_{2i} and $u_{i,\max}$ such that $\|u_i\|_\infty \leq u_{i,\max}$ and the Lyapunov function (17) for system (16) under the control input (3) satisfies $\dot{V}_i \leq 0$ if (24) and (25) hold.	Combine with (4), (5), (26) and (27) into (1), system (32) is obtained. Choose proper $\beta_{1i}, \beta_{2i}, \beta_{3i}$ and $u_{i,\max}$ such that $\|u_i\|_\infty \leq u_{i,\max}$, and the Lyapunov function (17) for system (32) under the control input (26) and Chain Rule satisfies $\dot{V}_i \leq 0$.
Step 4	Consequently, it follows that $e_i, \dot{e}_i$ are bounded with the upper bounds $\varepsilon_1, \varepsilon_2$ as $t \to \infty$, i.e. the PFT is realized.	Consequently, it follows that $e_i, \dot{e}_i \to 0$ as $t \to \infty$, i.e. the ZEFT is realized.

Assumption 3: System (1) is subjected to input constraints, that is, there exists a positive constant $u_{i,\max}$ without reference to model parameters, such that $\sup_{t\in T} \|u_i\|_\infty \leq u_{i,\max}$.

Assumption 4: The input disturbance term is bounded, that is, there exists a positive constant $\pi_{\kappa i}$, such that $\|\kappa_i\| \leq \pi_{\kappa i}$.

Control Objective: Design a controller to control a group of robotic agents initialized on random bounded positions to track the target in formation, that is, design control approaches to achieve the PFT and ZEFT for the considered multiple Euler–Lagrange systems in the sense of Definitions 1 and 2.

Definition 1: The PFT for system (1) is achieved, if for $\forall i \in \mathcal{N}$

$$\begin{cases} \lim_{t\to\infty} \| \tanh(q_i(t) - y_0(t) - \zeta_i)\| \leq \varepsilon_1 \\ \lim_{t\to\infty} \|\dot{q}_i(t) - z_0(t)\| \leq \varepsilon_2 \end{cases}$$

where ζ_i is a constant vector at time t, $\varepsilon_1 > 0$, $\varepsilon_2 > 0$.

Definition 2: The ZEFT for system (1) is achieved, if for $\forall i \in \mathcal{N}$

$$\begin{cases} \lim_{t\to\infty} \|q_i(t) - y_0(t) - \zeta_i\| = 0 \\ \lim_{t\to\infty} \|\dot{q}_i(t) - z_0(t)\| = 0. \end{cases}$$

Moreover, for all $i \in \mathcal{N}$, the following properties [58] are summarized for system (1).

Property 1: The matrix D_i is diagonal positive definite.

Property 2: The matrix $M_i(q_i)$ is symmetric positive definite.

Property 3: $\dot{M}_i(q_i) - 2C_i(q_i, \dot{q}_i)$ is skew-symmetric, that is, $\xi^T(\dot{M}_i(q_i) - 2C_i(q_i, \dot{q}_i))\xi = 0, \forall q_i, \dot{q}_i, \xi \in \mathcal{R}^n$.

Property 4: The dynamic items of system (1) are bounded, that is, $0 < \pi_{mi} \leq \|M_i(q_i)\| \leq \pi_{Mi}, 0 < \pi_{ci}\|\dot{q}_i\|^2 \leq \|C_i(q_i, \dot{q}_i)\dot{q}_i\| \leq \pi_{Ci}\|\dot{q}_i\|^2, 0 < \pi_{di} \leq \|D_i\| \leq \pi_{Di}, \|g_i(q_i)\| \leq \pi_{gi}$, and $\forall q_i, \dot{q}_i \in \mathcal{R}^n$, where $\pi_{mi}, \pi_{Mi}, \pi_{ci}, \pi_{Ci}, \pi_{Di}, \pi_{gi}$ are positive constants.

Finally, we give the following lemmas.

Lemma 1 [59]: If $\tau_1, \tau_2, \ldots, \tau_n \geq 0$ and $0 < \mu_1 < \mu_2$, then

$$\left(\sum_{i=1}^{n} \tau_i^{\mu_1}\right)^{1/\mu_1} \geq \left(\sum_{i=1}^{n} \tau_i^{\mu_2}\right)^{1/\mu_2}. \tag{2}$$

Lemma 2 [60]: If function $W(t) : [0, \infty) \to \mathcal{R}$ is uniformly continuous and $\lim_{t\to\infty} \int_0^t W(\epsilon)d\epsilon$ is finite, then $W(t) \to 0$ as $t \to \infty$.

III. MAIN RESULTS

In this section, we establish several conditions ensuring both the PFT and ZEFT for multiple Euler–Lagrange systems under two designed distributed and bounded control inputs. The control process of two bounded control inputs is displayed in Table I.

A. PFT Problem

For the PFT problem of system (1), the model-independent distributed control input is designed as follows:

$$u_i = \beta_{1i} \tanh(y_i - q_i) + \beta_{2i} \tanh(z_i - \dot{q}_i) \tag{3}$$

for $\forall i \in \mathcal{N}$, where β_{1i} and β_{2i} are positive constants. The estimated states y_i and z_i are given as

$$\dot{y}_i = -\eta_1 \text{sign}\left(\sum_{j\in\mathcal{N}_i} a_{ij}\big(y_i - \zeta_i - y_j + \zeta_j\big)\right) \tag{4}$$

$$\dot{z}_i = -\eta_2 \text{sign}\left(\sum_{j\in\mathcal{N}_i} a_{ij}\big(z_i - z_j\big)\right). \tag{5}$$

Then, the input is bounded by $\sup_{t\in T} \|u_i\|_\infty \leq \beta_{1i}+\beta_{2i}$, which means that the actuator saturation constraints can be fulfilled by choosing the control gains such that

$$\beta_{1i} + \beta_{2i} \leq u_{i,\max}. \tag{6}$$

Then, we define the estimated errors as

$$\bar{y}_i = y_i - y_0 - \zeta_i, \bar{z}_i = z_i - z_0$$

and the target tracking errors

$$e_i = q_i - y_0 - \zeta_i, \dot{e}_i = \dot{q}_i - z_0.$$

Remark 1: The bounded input constraints are considered in designing the control (3). With the introduction of the specific function tanh, it gives rise to the fact that the saturation upper bound is independent on the number of agents' neighbors. It shows that the presented control algorithm has advantages for the large-scale formation tracking systems, and is different from the saturated control methods in [51]–[57].

Remark 2: Actually, y_0 denotes the position coordinate of the time-varying target, and constant vector ζ_i represents the local coordinate in the formation pattern. The estimated states

Authorized licensed use limited to: IEEE Editors-in-Chief. Downloaded on June 14,2021 at 19:52:24 UTC from IEEE Xplore. Restrictions apply.

y_i and z_i are mainly introduced to estimate the states of the target, and are generated by the distributed estimators requiring only local information.

The following theorem shows the main result on achieving the PFT of multiple Euler–Lagrange systems under the control input (3).

Theorem 1: Based on Assumptions 1–4, the PFT is achieved by employing the control input (3), if there exist positive constants $\nu \geq 1$, β_{1i} and β_{2i} such that (6) holds, and for $i \in \mathscr{N}$

$$\nu^2\beta_{1i} - 2\pi_{Mi} > 0 \tag{7}$$

$$2\nu\pi_{di} - 2\pi_{Mi} - \left(2\sqrt{n} + 2\nu + 1\right)\pi_{Ci} > 0 \tag{8}$$

$$2\beta_{1i} - \beta_{2i} - \pi_{Ci} > 0. \tag{9}$$

Besides, the upper bounds ε_1 and ε_2 presented in Definition 1 are estimated as

$$\varepsilon_1 = \frac{2\delta_i}{2\beta_{1i} - \beta_{2i} - \pi_{Ci}} \tag{10}$$

$$\varepsilon_2 = \frac{2\nu\delta_i + 2\alpha_1\sqrt{n}\pi_{Ci}}{2\nu\pi_{di} - 2\pi_{Mi} - \left(2\sqrt{n} + 2\nu + 1\right)\pi_{Ci}} \tag{11}$$

where $\delta_i = \pi_{\kappa i} + \pi_{Mi}\alpha_2 + (\pi_{Ci} + \pi_{Di})\alpha_1 + \pi_{gi}$.

Proof: First, we can conclude that

$$\dot{\bar{y}}_i = -\eta_1 \mathrm{sign}\left(\sum_{j\in\mathcal{N}_i} a_{ij}\left(y_i - \zeta_i - y_j + \zeta_j\right)\right) - z_0 \tag{12}$$

$$\dot{\bar{z}}_i = -\eta_2 \mathrm{sign}\left(\sum_{j\in\mathcal{N}_i} a_{ij}\left(z_i - z_j\right)\right) - \dot{z}_0 \tag{13}$$

where $i \in \mathscr{N}$. Then, it results from [17] that $\bar{y}_i = \bar{z}_i = 0$ for all $t \geq t^* = \max\{t_1, t_2\}$, and

$$t_1 = t_0 + \frac{\max_{i\in\mathscr{N}} \|y_i(t_0) - y_0(t_0) - \zeta_i\|_\infty}{\eta_1 - \sup_{t\in T}\|z_0\|_\infty} \tag{14}$$

$$t_2 = t_0 + \frac{\max_{i\in\mathscr{N}} \|z_i(t_0) - z_0(t_0)\|_\infty}{\eta_2 - \sup_{t\in T}\|\dot{z}_0\|_\infty}. \tag{15}$$

Next, from (12) and (13), $y_0, z_0, \dot{z}_0 \in L_\infty \cap L_2$ means that $\dot{\bar{y}}_i, \dot{\bar{z}}_i \in L_\infty \cap L_2, \forall t \in [t_0, t^*], i \in \mathscr{N}$.

Thus, $y_i, z_i \in L_\infty \cap L_2$. Moreover, for any bounded initial conditions, it follows from Property 4 that $q_i, \dot{q}_i, e_i, \dot{e}_i \in L_\infty \cap L_2, \forall t \in [t_0, t^*], i \in \mathscr{N}$.

From system (1) and the control input (3), the following system can be obtained when $t \in [t^*, \infty)$:

$$\begin{aligned} &M_i(q_i)\ddot{e}_i + C_i(q_i, \dot{q}_i)\dot{e}_i + D_i\dot{e}_i \\ &\quad = \beta_{1i}\tanh(-e_i) + \beta_{2i}\tanh(-\dot{e}_i) + E_i \end{aligned} \tag{16}$$

where $E_i = \kappa_i - M_i(q_i)\dot{z}_0 - C_i(q_i, \dot{q}_i)z_0 - D_i z_0 - g_i(q_i)$ is bounded with $\|E_i\| \leq \delta_i + \pi_{Ci}\|\dot{e}_i\|$ and $\delta_i = \pi_{\kappa i} + \pi_{Mi}\alpha_2 + (\pi_{Ci} + \pi_{Di})\alpha_1 + \pi_{gi}$, $i \in \mathscr{N} = \{1, 2, \ldots, N\}$.

Then, consider the following Lyapunov function for system (16):

$$\begin{aligned} V_i = &\frac{1}{2}\dot{e}_i^T M_i(q_i)\dot{e}_i + \frac{1}{\nu}\tanh^T(e_i)M_i(q_i)\dot{e}_i \\ &+ \mathbf{1}_n^T\left(\beta_{1i}I + \frac{D_i}{\nu}\right)\ln(\cosh(e_i)) \end{aligned} \tag{17}$$

where $\nu \geq 1$ is a positive constant.

Note that

$$\begin{aligned} &\frac{1}{4}\dot{e}_i^T M_i(q_i)\dot{e}_i + \frac{1}{\nu}\tanh^T(e_i)M_i(q_i)\dot{e}_i \\ &= \frac{1}{4}\left(\dot{e}_i + \frac{2}{\nu}\tanh(e_i)\right)^T M_i(q_i)\left(\dot{e}_i + \frac{2}{\nu}\tanh(e_i)\right) \\ &\quad - \frac{1}{\nu^2}\tanh^T(e_i)M_i(q_i)\tanh(e_i) \\ &\geq -\frac{1}{\nu^2}\tanh^T(e_i)M_i(q_i)\tanh(e_i) \end{aligned} \tag{18}$$

and based on the definition of hyperbolic tangent and secant functions, the following inequalities can be derived:

$$\mathbf{1}_n^T\ln(\cosh(e_i)) \geq \frac{1}{2}\tanh^T(e_i)\tanh(e_i) \tag{19}$$

$$e_i^T\tanh(e_i) \geq \tanh^T(e_i)\tanh(e_i). \tag{20}$$

Then, it follows from (17)–(20) that:

$$\begin{aligned} V_i \geq &\frac{1}{4}\dot{e}_i^T M_i(q_i)\dot{e}_i - \frac{1}{\nu^2}\tanh^T(e_i)M_i(q_i)\tanh(e_i) \\ &+ \mathbf{1}_n^T\left(\beta_{1i}I + \frac{D_i}{\nu}\right)\ln(\cosh(e_i)) \\ \geq &\frac{1}{4}\dot{e}_i^T M_i(q_i)\dot{e}_i + \tanh^T(e_i)\left(\frac{\beta_{1i}}{2}I - \frac{M_i(q_i)}{\nu^2}\right)\tanh(e_i) \\ &+ \frac{1}{2}\tanh^T(e_i)\beta_{1i}\tanh(e_i) + \mathbf{1}_n^T\frac{D_i}{\nu}\ln(\cosh(e_i)) \\ > &\,0 \end{aligned} \tag{21}$$

for $\mathrm{col}(e_i^T \ \dot{e}_i^T) \neq 0$, which indicates that V_i is positive definite with respect to $e_i, \dot{e}_i$.

By calculating the time derivative of V_i along the solution of system (18), it follows that:

$$\begin{aligned} \dot{V}_i = &\frac{1}{2}\dot{e}_i^T\dot{M}_i(q_i)\dot{e}_i + \dot{e}_i^T M_i(q_i)\ddot{e}_i + \frac{1}{\nu}\dot{e}_i^T\mathrm{Sech}^2(e_i)M_i(q_i)\dot{e}_i \\ &+ \frac{1}{\nu}\tanh^T(e_i)\dot{M}_i(q_i)\dot{e}_i + \frac{1}{\nu}\tanh^T(e_i)M_i(q_i)\ddot{e}_i \\ &+ \dot{e}_i^T\left(\beta_{1i}I + \frac{D_i}{\nu}\right)\tanh(e_i) \\ = &\,\dot{e}_i^T(-D_i\dot{e}_i + \beta_{1i}\tanh(-e_i) + \beta_{2i}\tanh(-\dot{e}_i) + E_i) \\ &+ \frac{1}{\nu}\dot{e}_i^T\mathrm{Sech}^2(e_i)M_i(q_i)\dot{e}_i + \frac{1}{\nu}\tanh^T(e_i)C_i^T(q_i, \dot{q}_i)\dot{e}_i \\ &+ \frac{1}{\nu}\tanh^T(e_i)(-D_i\dot{e}_i + \beta_{1i}\tanh(-e_i) \\ &+ \beta_{2i}\tanh(-\dot{e}_i) + E_i) + \dot{e}_i^T\left(\beta_{1i}I + \frac{D_i}{\nu}\right)\tanh(e_i) \\ = &-\dot{e}_i^T D_i\dot{e}_i - \dot{e}_i^T\beta_{2i}\tanh(\dot{e}_i) + \dot{e}_i^T E_i + \frac{1}{\nu}\tanh^T(e_i)E_i \\ &+ \frac{1}{\nu}\dot{e}_i^T\mathrm{Sech}^2(e_i)M_i(q_i)\dot{e}_i + \frac{1}{\nu}\tanh^T(e_i)C_i^T(q_i, \dot{q}_i)\dot{e}_i \\ &- \frac{\beta_{1i}}{\nu}\tanh^T(e_i)\tanh(e_i) - \frac{\beta_{2i}}{\nu}\tanh^T(e_i)\tanh(\dot{e}_i). \end{aligned} \tag{22}$$

Based on Property 4, we have $\tanh^T(e_i)C_i^T(q_i, \dot{q}_i)\dot{e}_i \leq \pi_{Ci}(\alpha_1\|\dot{e}_i\| + \|\dot{e}_i\|^2)\|\tanh(e_i)\|$. Together with this inequality

Authorized licensed use limited to: IEEE Editors-in-Chief. Downloaded on June 14,2021 at 19:52:24 UTC from IEEE Xplore. Restrictions apply.

and $\|E_i\| \le \delta_i + \pi_{Ci}\|\dot{e}_i\|$, it follows from (22) that:

$$\begin{aligned}\dot{V}_i &\le -\dot{e}_i^T D_i \dot{e}_i - \tanh^T(\dot{e}_i)\beta_{2i}\tanh(\dot{e}_i) + \frac{\pi_{Mi}}{\nu}\|\dot{e}_i\|^2\\&\quad + \left(\dot{e}_i^T + \frac{1}{\nu}\tanh^T(e_i)\right)E_i + \frac{\sqrt{n}\pi_{Ci}\left(\alpha_1\|\dot{e}_i\| + \|\dot{e}_i\|^2\right)}{\nu}\\&\quad - \frac{\beta_{1i}}{\nu}\tanh^T(e_i)\tanh(e_i) - \frac{\beta_{2i}}{\nu}\tanh^T(e_i)\tanh(\dot{e}_i)\\&\le -\dot{e}_i^T D_i\dot{e}_i - \tanh^T(\dot{e}_i)\beta_{2i}\tanh(\dot{e}_i)\\&\quad + \frac{\pi_{Mi} + \sqrt{n}\pi_{Ci}}{\nu}\|\dot{e}_i\|^2 + \frac{\alpha_1\sqrt{n}\pi_{Ci}}{\nu}\|\dot{e}_i\|\\&\quad + \delta_i\|\dot{e}_i\| + \frac{\delta_i}{\nu}\|\tanh(e_i)\| + \pi_{Ci}\|\dot{e}_i\|^2\\&\quad + \frac{\pi_{Ci}}{\nu}\|\tanh(e_i)\|\|\dot{e}_i\| - \frac{\beta_{1i}}{\nu}\tanh^T(e_i)\tanh(e_i)\\&\quad + \frac{\beta_{2i}}{2\nu}\left(\|\tanh(e_i)\|^2 + \|\tanh(\dot{e}_i)\|^2\right)\\&\le -\left[\left(\pi_{di} - \frac{\pi_{Mi}}{\nu} - \left(\frac{\sqrt{n}}{\nu} + 1 + \frac{1}{2\nu}\right)\pi_{Ci}\right)\|\dot{e}_i\|\right.\\&\qquad \left. - \left(\delta_i + \frac{\alpha_1\sqrt{n}\pi_{Ci}}{\nu}\right)\right]\|\dot{e}_i\|\\&\quad - \left[\left(\frac{\beta_{1i}}{\nu} - \frac{\beta_{2i}}{2\nu} - \frac{\pi_{Ci}}{2\nu}\right)\|\tanh(e_i)\| - \frac{\delta_i}{\nu}\right]\|\tanh(e_i)\|\end{aligned} \tag{23}$$

where $\mathrm{Sech}(x_i) = \mathrm{diag}(\mathrm{sech}(x_{i1}), \ldots, \mathrm{sech}(x_{in}))$.

One can conclude that $\dot{V}_i \le 0$ if

$$\|\dot{e}_i\| > \frac{2\nu\delta_i + 2\alpha_1\sqrt{n}\pi_{Ci}}{2\nu\pi_{di} - 2\pi_{Mi} - \left(2\sqrt{n} + 2\nu + 1\right)\pi_{Ci}} \tag{24}$$

$$\|\tanh(e_i)\| > \frac{2\delta_i}{2\beta_{1i} - \beta_{2i} - \pi_{Ci}}. \tag{25}$$

Then, the PFT is realized, which completes the proof. ■

Remark 3: Theorem 1 solves the PFT problem for multiple Euler–Lagrange systems subjected to the bounded input constraints and provides the fact that using the designed control law (3), the errors between the system states and the time-varying target trajectories converge to a neighborhood of the origin. Then, it can be concluded from (10) and (11) that choosing large enough gain β_{1i} leads to an arbitrary small upper bound ε_1 if ε_2 is fixed. It further implies that the robot position q_i can be arbitrarily close to $y_0 + \zeta_i$ as $t \to \infty$.

Remark 4: Actually, the proposed model-independent controllers do not rely on the exact knowledge of the model parameters. To achieve PFT using such controllers, the boundaries of the control gains are obtained by employing the trial-and-error method [48], and this method has already been processed in many existing papers considering the model-independent algorithms.

B. ZEFT Problem

To improve the convergence performance of the PFT and realize the ZEFT, another discontinuous control input is proposed in this section. Before moving on, the model-independent control is designed as follows:

$$u_i = \beta_{1i}\tanh(y_i - q_i) + \beta_{2i}\tanh(z_i - \dot{q}_i) + \beta_{3i}\mathrm{sign}(\omega_i) \tag{26}$$

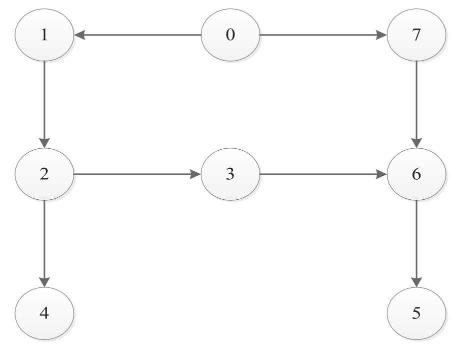

Fig. 1. Directed communication graph of multiple Euler–Lagrange systems as described in (35).

where

$$\omega_i = (z_i - \dot{q}_i) + 1/\nu\tanh(y_i - q_i) \tag{27}$$

for $\forall i \in \mathcal{N}$, $\nu \ge 1$, β_{3i} are positive constants, and the other parameters are defined as the same as in (3). Then, the actuator is bounded, that is, $\sup_{t\in T}\|u_i\|_\infty \le \beta_{1i} + \beta_{2i} + \beta_{3i}$, which implies that the bounded input constraints can be fulfilled by choosing the control gains such that

$$\beta_{1i} + \beta_{2i} + \beta_{3i} \le u_{i,\max}. \tag{28}$$

Remark 5: Since the designed control input (26) is discontinuous, then the Filippov solution [61] is defined for the system (1) with such discontinuous control. A solution in the Filippov's sense of system $\dot{x} = h(t, x), x(0) = x_0, x \in \mathcal{R}^n, t \ge 0$ is defined as an absolutely continuous function $x(t), t \in [0, T], T > 0$, which satisfies $x(0) = x_0$, and for almost all (a.a.) $t \in [0, T]$, the differential inclusion $\dot{x} \in \Lambda(t, x)$ holds, where $\Lambda(t, x) = \bigcap_{\phi>0}\bigcap_{\mu(\Delta)=0}\overline{co}[h(t, B(x, \phi)\backslash\Delta)]$, $\overline{co}$ is the convex closure hull, $B(x, \delta)$ is the open ball of center x with radius ϕ, and $\Delta \subset \mathcal{R}^n$, $\mu(\Delta)$ is the Lebesgue measure of set Δ.

The following theorem is presented to show the ZEFT of multiple Euler–Lagrange systems using the control input (26).

Theorem 2: Based on Assumptions 1–4, the ZEFT is achieved by employing control input (26), if there exists positive constants $\nu \ge 1$, β_{1i}, β_{2i}, β_{3i} such that (7) and (28) hold, and for $\forall i \in \mathcal{N}$

$$2\nu\pi_{di} - 2\pi_{Mi} - \left(\alpha_1 + 2\sqrt{n} + 2\nu + 1\right)\pi_{Ci} > 0 \tag{29}$$

$$2\beta_{1i} - (\alpha_1 + 1)\pi_{Ci} - \beta_{2i} > 0 \tag{30}$$

$$\beta_{3i} - \delta_i > 0. \tag{31}$$

Proof: It also comes to the conclusion that $\bar{y}_i = \bar{z}_i = 0$ for all $t \ge t^* = \max\{t_1, t_2\}$, and $q_i, \dot{q}_i, e_i, \dot{e}_i \in L_\infty \cap L_2, \forall t \in [t_0, t^*], i \in \mathcal{N}$.

From system (1) and the control input (26), the following system can be obtained when $t \in [t^*, \infty)$:

$$\begin{aligned}&M_i(q_i)\ddot{e}_i + C_i(q_i, \dot{q}_i)\dot{e}_i + D_i\dot{e}_i\\&\quad = \beta_{1i}\tanh(-e_i) + \beta_{2i}\tanh(-\dot{e}_i) + \beta_{3i}\mathrm{sign}(-x_i) + E_i\end{aligned} \tag{32}$$

where $x_i = \dot{e}_i + 1/\nu\tanh(e_i)$, $i \in \mathcal{N}$.

Considering the same Lyapunov function (17), it follows from Theorem 1 that V_i is positive definite with respect to $e_i, \dot{e}_i$.

Authorized licensed use limited to: IEEE Editors-in-Chief. Downloaded on June 14,2021 at 19:52:24 UTC from IEEE Xplore. Restrictions apply.

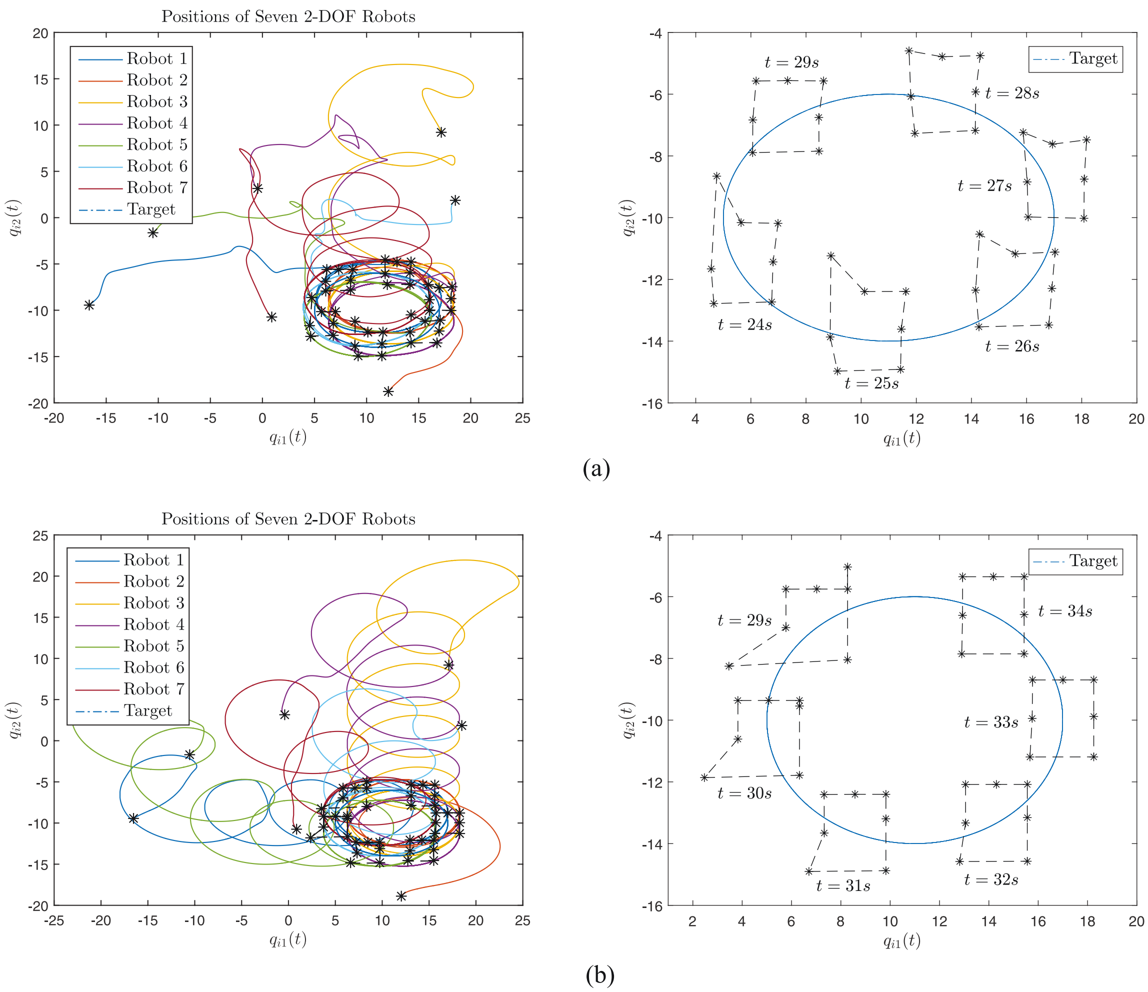

Fig. 2. Formation tracking performances of seven robots under control inputs (a) (3) and (b) (26). The thumbnail right is six time points at which the tracking performances are distinctly presented.

Under the chain rule [62], the time derivative of V_i, along the solution of system (32), exists for a.a. $t \in [t_0, \infty)$, that is

$$\begin{aligned}\dot{V}_i \overset{\text{a.a.}}{\in}\; & \dot{e}_i^T(-D_i\dot{e}_i + \beta_{1i}\tanh(-e_i) + \beta_{2i}\tanh(-\dot{e}_i)\\ & + \beta_{3i}\mathrm{SIGN}(-x_i) + E_i) + \frac{1}{\nu}\dot{e}_i^T\mathrm{Sech}^2(e_i)M_i(q_i)\dot{e}_i\\ & + \frac{1}{\nu}\tanh^T(e_i)C_i^T(q_i,\dot{q}_i)\dot{e}_i + \frac{1}{\nu}\tanh^T(e_i)(-D_i\dot{e}_i\\ & + \beta_{1i}\tanh(-e_i) + \beta_{2i}\tanh(-\dot{e}_i) + \beta_{3i}\mathrm{SIGN}(-x_i)\\ & + E_i) + \dot{e}_i^T\left(\beta_{1i}I + \frac{D_i}{\nu}\right)\tanh(e_i)\end{aligned} \tag{33}$$

where $\mathrm{SIGN}(x_i) = 1$ if $x_i > 0$, $[-1, 1]$ if $x_i = 0$, and -1 if $x_i < 0$. Then, it follows that for a.a. $t \in [t_0, \infty)$:

$$\begin{aligned}\dot{V}_i \le\; & -\dot{e}_i^T D_i\dot{e}_i - \tanh^T(\dot{e}_i)\beta_{2i}\tanh(\dot{e}_i) - \beta_{3i}\|x_i\|_1\\ & + \left(\dot{e}_i^T + \frac{1}{\nu}\tanh^T(e_i)\right)E_i + \frac{\pi_{Mi}}{\nu}\|\dot{e}_i\|^2\\ & + \frac{\sqrt{n}\pi_{Ci}}{\nu}\|\dot{e}_i\|^2 + \frac{\alpha_1\pi_{Ci}}{2\nu}\left(\|\tanh(e_i)\|^2 + \|\dot{e}_i\|^2\right)\\ & - \frac{\beta_{1i}}{\nu}\tanh^T(e_i)\tanh(e_i) - \frac{\beta_{2i}}{\nu}\tanh^T(e_i)\tanh(\dot{e}_i)\\ \le\; & -\left[\pi_{di} - \frac{\pi_{Mi}}{\nu} - \left(\frac{\alpha_1}{2\nu} + \frac{\sqrt{n}}{\nu}\right)\pi_{Ci}\right]\|\dot{e}_i\|^2\\ & - \left(\beta_{2i} - \frac{\beta_{2i}}{2\nu}\right)\|\tanh(\dot{e}_i)\|^2\\ & - \frac{1}{2\nu}(2\beta_{1i} - \alpha_1\pi_{Ci} - \beta_{2i})\|\tanh(e_i)\|^2\\ & + \|\dot{e}_i + 1/\nu\tanh(e_i)\|(\delta_i + \pi_{Ci}\|\dot{e}_i\|) - \beta_{3i}\|x_i\|_1\\ \le\; & -\left[\pi_{di} - \frac{\pi_{Mi}}{\nu} - \left(\frac{\alpha_1}{2\nu} + \frac{\sqrt{n}}{\nu} + 1 + \frac{1}{2\nu}\right)\pi_{Ci}\right]\|\dot{e}_i\|^2\\ & - \frac{1}{2\nu}(2\beta_{1i} - (\alpha_1 + 1)\pi_{Ci} - \beta_{2i})\|\tanh(e_i)\|^2\\ & - (\beta_{3i} - \delta_i)\|x_i\|\\ \le\; & 0.\end{aligned} \tag{34}$$

It follows from (19), (32), and (34) that $e_i, \dot{e}_i \in L_\infty \cap L_2$. Thus, $x_i, E_i, \ddot{e}_i \in L_\infty \cap L_2$. By Lemma 2 and [62, Corollary 1], it comes to the conclusion that $e_i \to 0, \dot{e}_i \to 0$ as $t \to \infty$, which means that the ZEFT is realized. Then, the proof is completed. ■

Remark 6: Different from [49], in which the prior information of the accurate model of the Euler–Lagrange

Authorized licensed use limited to: IEEE Editors-in-Chief. Downloaded on June 14,2021 at 19:52:24 UTC from IEEE Xplore. Restrictions apply.

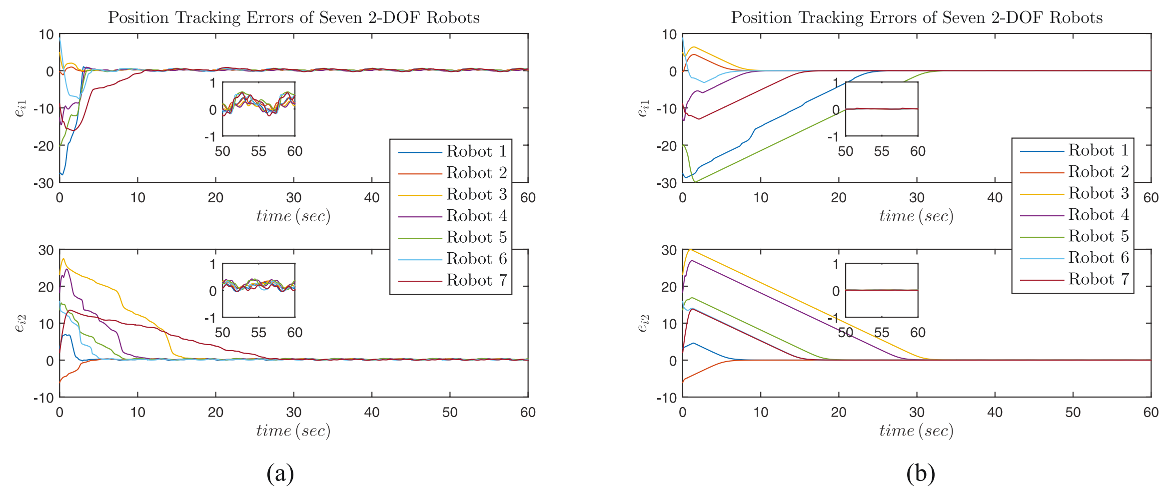

Fig. 3. Tracking performances of positions under saturated control inputs (a) (3) and (b) (26).

systems is required, the presented model-independent control approaches in this article do not require the knowledge of system models, which show the superiority of model-independent control.

Remark 7: The results in this article improve those in [18], [19], and [50] in the following two aspects. First, Theorems 1 and 2 address both the PFT and ZEFT problems under two classes of control inputs while only the PFT problem was studied in [18] and [19]. Second, bounded input constraints are considered in designing the control laws, which can reduce the control cost for large-scale systems like the multiple Euler–Lagrange systems in [50].

Remark 8: Under bounded input constraints, zero-error consensus may be hard to access and only practical consensus (semiglobal consensus) was obtained in [52]–[56]. Since both the PFT and ZEFT are successfully addressed in this article, our results can be seen as the extension of those in [52]–[56] where only practical consensus was achieved.

Remark 9: Compared with the existing formation tracking studies of the nonlinear Euler–Lagrange systems in [16], [18]–[20], [39], and [49], the formation tracking results and the designed control input in this article show the superiorities as follows.

1) From the physical point of view, the time-varying tracking target, input disturbances can represent more realistic prospects.
2) Both the PFT and ZEFT are obtained simultaneously and they can meet corresponding unsolved and wider practical requirements.
3) The control input with boundedness constraints can save control cost, especially for large system states.
4) The distributed and model-independent control inputs can be employed to deal with control systems with limited model information and provide theoretical guidance for such problems.

Remark 10: In Theorems 1 and 2, it is not apparent how to select the control gains since they rely on the dynamic matrices D_i, M_i, C_i of system (1). By using the MATLAB toolbox, the boundary of these control gains can be obtained by

TABLE II
VALUES OF THE INTERIM PARAMETERS FOR SEVEN ROBOTIC AGENTS

	robot 1	robot 2	robot 3	robot 4	robot 5	robot 6	robot 7
h_1	0.1710	0.2076	0.2483	0.2931	0.3423	0.3959	0.4540
h_2	0.0661	0.0795	0.0943	0.1105	0.1283	0.1475	0.1682
h_3	0.0540	0.0649	0.0770	0.0903	0.1047	0.1204	0.1374
a	0.3855	0.4230	0.4795	0.5280	0.5775	0.6280	0.6795
b	0.3003	0.3312	0.3267	0.3948	0.4275	0.4608	0.4947

the trial-and-error method [48]. Then, the estimated feasible region H_i in Theorem 1 and G_i in Theorem 2 can be described, respectively, as

$$H_i = \Big\{(\beta_{1i}, \beta_{2i}) \in \mathcal{R}_+ \times \mathcal{R}_+ | \beta_{1i} + \beta_{2i} \le u_{i,\max} \\ \beta_{1i} > \frac{2\pi_{Mi}}{\nu^2}, 0 < \beta_{2i} < 2\beta_{1i} - \pi_{Ci}\Big\}$$

and

$$G_i = \Big\{(\beta_{1i}, \beta_{2i}, \beta_{3i}) \in \mathcal{R}_+ \times \mathcal{R}_+ | \beta_{1i} + \beta_{2i} + \beta_{3i} \le u_{i,\max} \\ \beta_{1i} > \frac{2\pi_{Mi}}{\nu^2}, 0 < \beta_{2i} < 2\beta_{1i} - (\alpha_1 + 1)\pi_{Ci}, \beta_{3i} > \delta_i\Big\}$$

for $i \in \mathcal{N}$.

IV. Numerical Simulations

In this section, seven robotic agents are considered to show the formation tracking problem of multiple Euler–Lagrange systems, the dynamics of each two-DOF robot manipulator [58] is as follows:

$$\begin{bmatrix} M_{i1} & M_{i2} \\ M_{i2} & M_{i3} \end{bmatrix} \begin{bmatrix} \ddot{q}_{i1} \\ \ddot{q}_{i2} \end{bmatrix} + \begin{bmatrix} C_{i1} & C_{i2} \\ C_{i3} & C_{i4} \end{bmatrix} \begin{bmatrix} \dot{q}_{i1} \\ \dot{q}_{i2} \end{bmatrix} \\ + \begin{bmatrix} D_{i1} & 0 \\ 0 & D_{i2} \end{bmatrix} \begin{bmatrix} \dot{q}_{i1} \\ \dot{q}_{i2} \end{bmatrix} + \begin{bmatrix} g_{i1} \\ g_{i2} \end{bmatrix} = \begin{bmatrix} u_{i1} \\ u_{i2} \end{bmatrix} + \begin{bmatrix} \kappa_{i1} \\ \kappa_{i2} \end{bmatrix} \quad (35)$$

Authorized licensed use limited to: IEEE Editors-in-Chief. Downloaded on June 14,2021 at 19:52:24 UTC from IEEE Xplore. Restrictions apply.

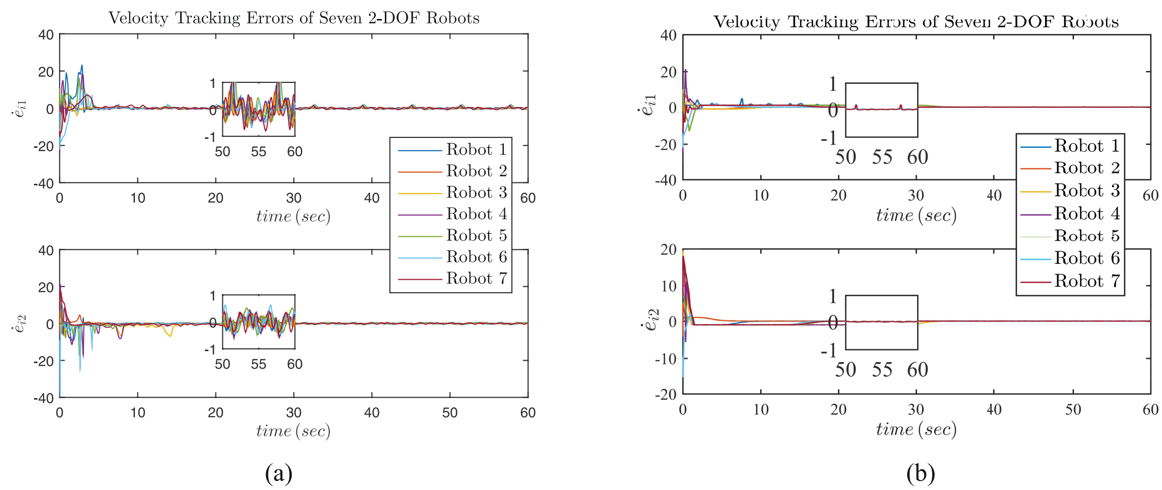

Fig. 4. Tracking performances of velocities under saturated control inputs (a) (3) and (b) (26).

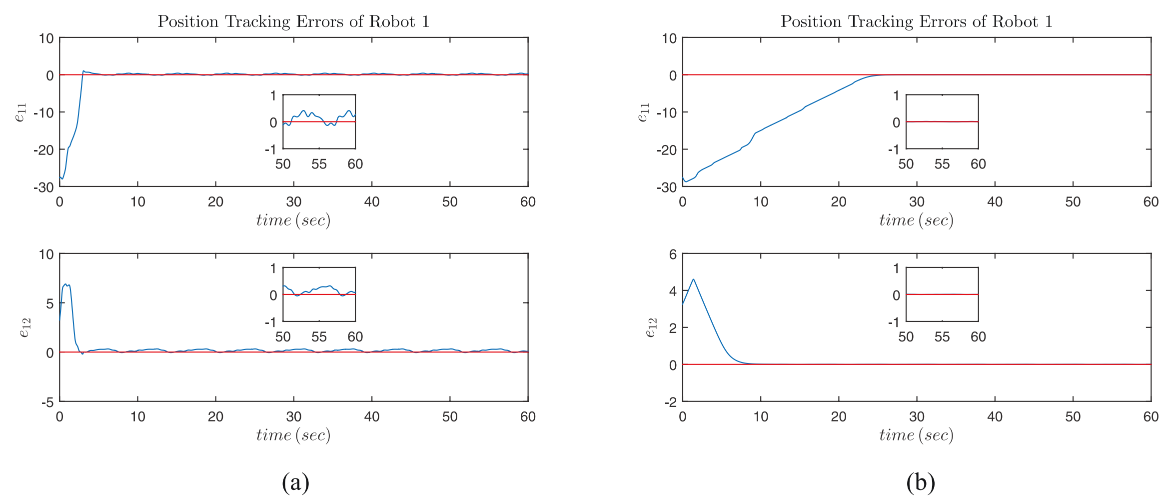

Fig. 5. Position tracking errors of robot 1 under saturated control inputs (a) (3) and (b) (26).

where the model parameters for each manipulator are $M_{i1} = h_{i1} + 2h_{i2}\cos q_{i2}, M_{i2} = h_{i3} + h_{i2}\cos q_{i2}, M_{i3} = h_{i3}, C_{i1} = -h_{i2}\sin q_{i2}\dot{q}_{i2}, C_{i2} = -h_{i2}\sin q_{i2}(\dot{q}_{i1} + \dot{q}_{i2}), C_{i3} = h_{i2}\sin q_{i2}\dot{q}_{i1}, C_{i4} = 0, g_{i1} = ag\cos q_{i1} + g_{i2}, g_{i2} = bg\cos(q_{i1} + q_{i2}), h_{i2} = m_{i2}f_{i1}l_{i2}, h_{i3} = m_{i2}l_{i2}^2 + Q_{i2}, h_{i1} = m_{i1}l_{i1}^2 + m_{i2}(f_{i1}^2 + l_{i2}^2) + Q_{i1} + Q_{i2}, a = m_{i1}l_{i1} + m_{i2}f_{i1}, b = m_{i2}f_{i2}, i = 1, \ldots, 7$, and g = 9.8 m/s^2 is the gravitational acceleration, $m_{is}, l_{is}, f_{is}, Q_{is} (s = 1, 2, i = 1, \ldots, 7)$ denote the mass and distance from the previous joint to the center, length, and moment of inertia of the sth link of the $i$the robot manipulator.

Without loss of generality, set $m_{i1} = 0.7 + 0.01i, l_{i1} = 0.1 + 0.02i, f_{i1} = 0.3 + 0.03i, Q_{i1} = m_{i1}f_{i1}^2/10, m_{i2} = 0.9 + 0.01i, l_{i2} = 0.2 + 0.02i, f_{i2} = 0.3 + 0.03i, Q_{i2} = m_{i2}f_{i2}^2/10$ for $i = 1, \ldots, 7$. Then, choose $D_{11} = 1.5, D_{21} = 1.2, D_{31} = 1, D_{41} = 1.3, D_{51} = 1.4, D_{61} = 1.7, D_{71} = 1.4, D_{12} = 1, D_{22} = 1.6, D_{32} = 1.7, D_{42} = 1.5, D_{52} = 1.3, D_{62} = 1.2, D_{72} = 1.6$, and the disturbances are given as $\kappa_{i1} = 5|\sin(t)|, \kappa_{i2} = 5|\cos(t)|, t \geq t_0 = 0$. Then, it follows Table II by simple calculation. The directed communication graph of seven robots and the target (node 0) are provided in Fig. 1. The trajectory of the time-varying target and the formation patterns are given as $y_0(t) = \mathrm{col}(11 + 6\sin(t), -10 - 4\cos(t))$, $\zeta_1 = (0, 1.25)^T, \zeta_2 = (1.25, 1.25)^T, \zeta_3 = (1.25, 0)^T, \zeta_4 = (1.25, -1.25)^T, \zeta_5 = (-1.25, -1.25)^T, \zeta_6 = (-1.25, 0)^T$, and $\zeta_7 = (-1.25, 1.25)^T$.

TABLE III
SELECTED CONTROL GAINS

	i = 1	i = 2	i = 3	i = 4	i = 5	i = 6	i = 7
β_{1i}	15	18	20	15	17	16	20
β_{2i}	20	15	20	17	18	20	13
β_{3i}	15	20	18	20	20	20	17

To ensure that the upper bound of the tracking performance in Definition 1 is less enough to fulfil the practical requirement, the boundaries of the control gains are given large enough and mainly vary from 15 to 20. For control inputs (3) and (26), the bounded input constraints are given as 40 and 60, respectively. Based on the derived criteria in Theorems 1 and 2, and the feasible regions in Remark 10, the control gains in (3) and (26) are chosen as in Table III. Then, it can be concluded that the PFT and ZEFT problems are solved for seven

Authorized licensed use limited to: IEEE Editors-in-Chief. Downloaded on June 14,2021 at 19:52:24 UTC from IEEE Xplore. Restrictions apply.

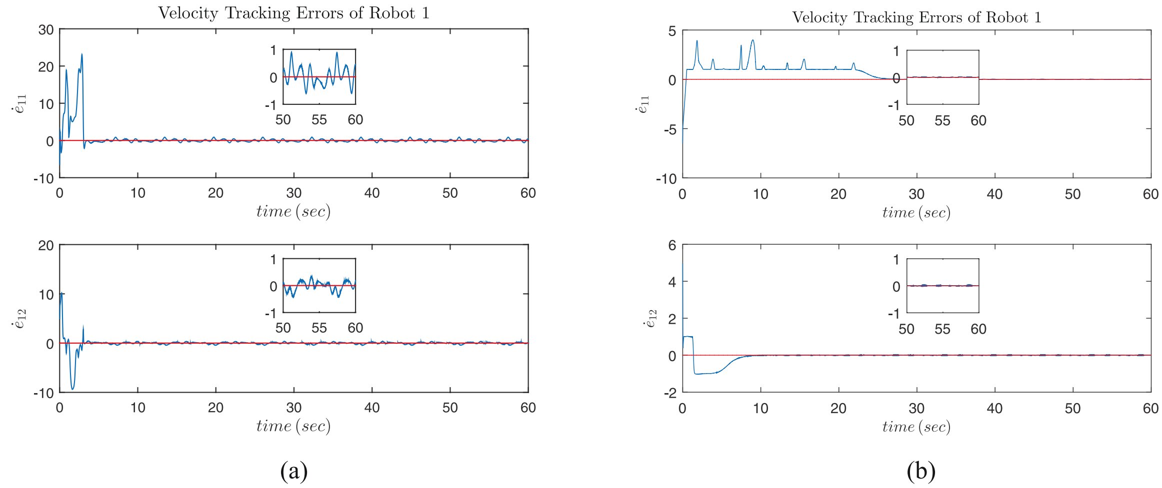

Fig. 6. Velocity tracking errors of robot 1 under saturated control inputs (a) (3) and (b) (26).

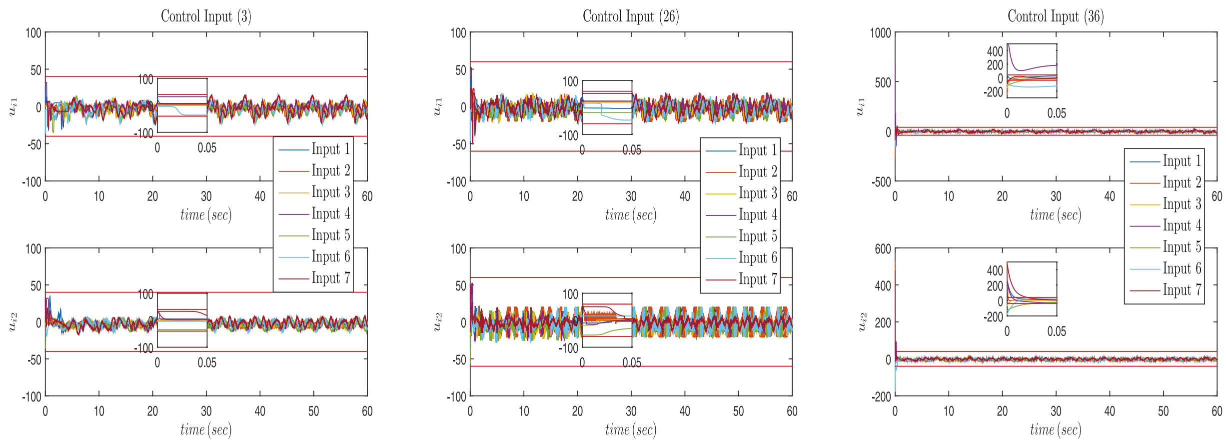

Fig. 7. Trajectories of saturated control inputs (3) and (26), and unsaturated control input (36).

robots (35). Fig. 2 shows the formation tracking performances of seven robots under control inputs (3) and (26). We also give six time points at which the tracking performances are distinctly presented. It can be seen from Fig. 2 that seven robots will tend to an orderly formation following the target.

Given arbitrary initial conditions (each entry of the initial states is bounded in $[-20, 20]$), the formation tracking performances of positions q_{i1}, q_{i2} and velocities $\dot{q}_{i1}, \dot{q}_{i2}$ using control inputs (3) and (26) are shown in Figs. 3 and 4, respectively. From Figs. 3 and 4, it can be seen that by employing the control input (3), the position and velocity tracking errors are bounded and converge to a neighborhood of the origin as time goes to infinite, while under the control input (26), the tracking errors tend to zero as time goes to infinite. Thus, it can be concluded that the control input (26) possesses better formation tracking performance compared to control input (3), which also reveals the superiority for implementing the ZEFT of multiple Euler–Lagrange systems. To show the performance of the tracking errors clearly, we further present the position and velocity tracking errors by considering just robot 1 since other tracking errors for robots 2–7 are similarly obtained. Then, for robot 1 under control inputs (3) and (26), Figs. 5 and 6 depict, respectively, the position and velocity tracking errors.

To show the different functions of saturated (bounded) and unsaturated control approaches, we give the following unsaturated control input. Its formation tracking performances are omitted since they are similar to the ones in Figs. 3(a)–6(a)

$$u_i = \beta_{1i}(y_i - q_i) + \beta_{2i}(z_i - \dot{q}_i) \tag{36}$$

for $\forall i \in \mathcal{N}$, where β_{1i} and β_{2i} are positive constants. Fig. 7 depicts the trajectories of saturated control inputs (3) and (26), and unsaturated control input (36). From Fig. 7, we can see that the saturated control inputs (3) and (26) are subjected to the saturation constraints and they remain bounded as time goes from zero to infinite. However, the control gains of the unsaturated control input (36) can be very large at the beginning time. To this extent, the saturated control approaches adopted in this article show the superiority for the reduction of control cost.

Remark 11: Together with Figs. 3–7, it is concluded that both saturated (bounded) and unsaturated control inputs can be adopted to carry out the PFT and ZEFT. However, there are two main differences for them.

Authorized licensed use limited to: IEEE Editors-in-Chief. Downloaded on June 14,2021 at 19:52:24 UTC from IEEE Xplore. Restrictions apply.

1) The control input with saturation constraints can save control cost, especially for large system states. As we can see from Fig. 7, all trajectories of saturated control inputs (3) and (26) remain under the saturation constraints 40 and 60, respectively, while the trajectories of unsaturated control input (36) are very large in the first few seconds.
2) The convergence speed of saturated control inputs is slower than the unsaturated one at the expense of lower control cost. Still, we can adopt the saturated control input (26) instead of (3) to obtain better tracking performance.

V. Conclusion

For multiple Euler–Lagrange systems with directed interaction graphs and input disturbances, the formation tracking problems, including the PFT problem and ZEFT problem, have been fully addressed. Two model-independent distributed control laws under the bounded input constraints have been proposed to solve the PFT and ZEFT problem. The presented distributed control laws do not require prior information of structures and features of the system model, and can provide robustness against input disturbances. In addition, the input upper bound of the two approaches is independent of the number of agents' neighbors. These unique characteristics of the presented control laws show their superiority, which has been verified by carrying out comparison studies in both discussions and simulations. Then, the corresponding criteria for practical and asymptotic stability of the presented bounded control algorithms have been derived. In this article, we mainly consider how to realize constant formation tracking. Future work will focus on the inter-robot collisions and the time-varying formation tracking problem of multiple Euler–Lagrange systems. Moreover, such systems with stochastic noises and other uncertainties can also be a good choice.

References

[1] W. Ren and R. W. Beard, *Distributed Consensus in Multi-Vehicle Cooperative Control*. London, U.K.: Springer-Verlag, 2008.

[2] Z. Lin, B. Francis, and M. Maggiore, "Necessary and sufficient graphical conditions for formation control of unicycles," *IEEE Trans. Autom. Control*, vol. 50, no. 1, pp. 121–127, Jan. 2005.

[3] P. Wang and B. Ding, "Distributed RHC for tracking and formation of nonholonomic multi-vehicle systems," *IEEE Trans. Autom. Control*, vol. 59, no. 6, pp. 1439–1453, Jun. 2014.

[4] T. Han, Z.-H. Guan, B. Xiao, J. Wu, and X. Chen, "Distributed output consensus of heterogeneous multi-agent systems via an output regulation approach," *Neurocomputing*, vol. 360, pp. 131–137, Sep. 2019.

[5] Z.-W. Liu, Z.-H. Guan, X. Shen, and G. Feng, "Consensus of multi-agent networks with aperiodic sampled communication via impulsive algorithms using position-only measurements," *IEEE Trans. Autom. Control*, vol. 57, no. 10, pp. 2639–2643, Oct. 2012.

[6] X.-S. Zhan, L.-L. Cheng, J. Wu, Q.-S. Yang, and T. Han, "Optimal modified performance of MIMO networked control systems with multi-parameter constraints," *ISA Trans.*, vol. 84, pp. 111–117, Jan. 2019.

[7] X. Dong and G. Hu, "Time-varying formation tracking for linear multiagent systems with multiple leaders," *IEEE Trans. Autom. Control*, vol. 62, no. 7, pp. 3658–3664, Jul. 2017.

[8] G. Wen, W. Yu, Z. Li, X. Yu, and J. Cao, "Neuro-adaptive consensus tracking of multiagent systems with a high-dimensional leader," *IEEE Trans. Cybern.*, vol. 47, no. 7, pp. 1730–1742, Jul. 2017.

[9] S. S. Ge, X. Liu, C. H. Goh, and L. Xu, "Formation tracking control of multiagents in constrained space," *IEEE Trans. Control Syst. Technol.*, vol. 24, no. 3, pp. 992–1003, May 2016.

[10] L. Wang, H. He, and Z. Zeng, "Global synchronization of fuzzy memristive neural networks with discrete and distributed delays," *IEEE Trans. Fuzzy Syst.*, to be published. doi: 10.1109/TFUZZ.2019.2930032.

[11] X. Liang, Y.-H. Liu, H. Wang, W. Chen, K. Xing, and T. Liu, "Leader-following formation tracking control of mobile robots without direct position measurements," *IEEE Trans. Autom. Control*, vol. 61, no. 12, pp. 4131–4137, Dec. 2016.

[12] H. Liu, T. Ma, F. L. Lewis, and Y. Wan, "Robust formation control for multiple quadrotors with nonlinearities and disturbances," *IEEE Trans. Cybern.*, to be published. doi: 10.1109/TCYB.2018.2875559.

[13] M.-F. Ge, Z.-W. Liu, G. Wen, X. Yu, and T. Huang, "Hierarchical controller-estimator for coordination of networked Euler–Lagrange systems," *IEEE Trans. Cybern.*, to be published. doi: 10.1109/TCYB.2019.2914861.

[14] L. Wang, T. Dong, and M. F. Ge, "Finite-time synchronization of memristor chaotic systems and its application in image encryption," *Appl. Math. Comput.*, vol. 347, pp. 293–305, Apr. 2019.

[15] S. Zuo, Y. Song, F. L. Lewis, and A. Davoudi, "Adaptive output formation-tracking of heterogeneous multi-agent systems using time-varying $\mathcal{L}_2$-gain design," *IEEE Control Syst. Lett.*, vol. 2, no. 2, pp. 236–241, Apr. 2018.

[16] X. Dong, Y. Zhou, Z. Ren, and Y. Zhong, "Time-varying formation tracking for second-order multi-agent systems subjected to switching topologies with application to quadrotor formation flying," *IEEE Trans. Ind. Electron.*, vol. 64, no. 6, pp. 5014–5024, Jun. 2017.

[17] Y. Cao, W. Ren, and Z. Meng, "Decentralized finite-time sliding mode estimators and their applications in decentralized finite-time formation tracking," *Syst. Control Lett.*, vol. 59, no. 9, pp. 522–529, Sep. 2010.

[18] J. Yu, X. Dong, Q. Li, and Z. Ren, "Practical time-varying formation tracking for second-order nonlinear multiagent systems with multiple leaders using adaptive neural networks," *IEEE Trans. Neural Netw. Learn. Syst.*, vol. 29, no. 12, pp. 6015–6025, Dec. 2018.

[19] J. Yu, X. Dong, Z. Liang, Q. Li, and Z. Ren, "Practical time-varying formation tracking for high-order nonlinear multiagent systems with multiple leaders based on the distributed disturbance observer," *Int. J. Robust Nonlinear Control*, vol. 28, no. 9, pp. 3258–3272, Jun. 2018.

[20] Y. Hua, X. Dong, Q. Li, and Z. Ren, "Distributed time-varying formation robust tracking for general linear multiagent systems with parameter uncertainties and external disturbances," *IEEE Trans. Cybern.*, vol. 47, no. 8, pp. 1959–1969, Aug. 2017.

[21] F. Chen and W. Ren, "A connection between dynamic region-following formation control and distributed average tracking," *IEEE Trans. Cybern.*, vol. 48, no. 6, pp. 1760–1772, Jun. 2018.

[22] Y. Cao, W. Yu, W. Ren, and G. Chen, "An overview of recent progress in the study of distributed multi-agent coordination," *IEEE Trans. Ind. Inf.*, vol. 9, no. 1, pp. 427–438, Feb. 2013.

[23] Z.-G. Hou, "A hierarchical optimization neural network for large-scale dynamic systems," *Automatica*, vol. 37, no. 12, pp. 1931–1940, Dec. 2001.

[24] Z. Meng, Z. Lin, and W. Ren, "Leader–follower swarm tracking for networked Lagrange systems," *Syst. Control Lett.*, vol. 61, no. 1, pp. 117–126, Jan. 2012.

[25] Z. Meng, D. V. Dimarogonas, and K. H. Johansson, "Leader–follower coordinated tracking of multiple heterogeneous Lagrange systems using continuous control," *IEEE Trans. Robot.*, vol. 30, no. 3, pp. 739–745, Jun. 2014.

[26] C. Ma, P. Shi, X. Zhao, and Q. Zeng, "Consensus of Euler–Lagrange systems networked by sampled-data information with probabilistic time delays," *IEEE Trans. Cybern.*, vol. 45, no. 6, pp. 1126–1133, Jun. 2015.

[27] G. Chen, Y. Song, and F. L. Lewis, "Distributed fault-tolerant control of networked uncertain Euler–Lagrange systems under actuator faults," *IEEE Trans. Cybern.*, vol. 47, no. 7, pp. 1706–1718, Jul. 2017.

[28] F. Chen, G. Feng, L. Liu, and W. Ren, "Distributed average tracking of networked Euler–Lagrange systems," *IEEE Trans. Autom. Control*, vol. 60, no. 2, pp. 547–552, Feb. 2015.

[29] J. Mei, W. Ren, and G. Ma, "Distributed coordinated tracking with a dynamic leader for multiple Euler–Lagrange systems," *IEEE Trans. Autom. Control*, vol. 56, no. 6, pp. 1415–1421, Jun. 2011.

[30] Y. Zhao, Z. Duan, and G. Wen, "Distributed finite-time tracking of multiple Euler–Lagrange systems without velocity measurements," *Int. J. Robust Nonlinear Control*, vol. 25, no. 11, pp. 1688–1703, Jul. 2015.

[31] X. Zhao, X. Zheng, C. Ma, and R. Li, "Distributed consensus of multiple Euler–Lagrange systems networked by sampled-data information with transmission delays and data packet dropouts," *IEEE Trans. Autom. Sci. Eng.*, vol. 14, no. 3, pp. 1440–1450, Jul. 2017.

[32] J. R. Klotz, S. Obuz, Z. Kan, and W. E. Dixon, "Synchronization of uncertain Euler–Lagrange systems with uncertain time-varying communication delays," *IEEE Trans. Cybern.*, vol. 48, no. 2, pp. 807–817, Feb. 2018.

[33] H. Wang, "Flocking of networked uncertain Euler–Lagrange systems on directed graphs," *Automatica*, vol. 49, no. 9, pp. 2774–2779, Sep. 2013.

Authorized licensed use limited to: IEEE Editors-in-Chief. Downloaded on June 14,2021 at 19:52:24 UTC from IEEE Xplore. Restrictions apply.

[34] G. Chen, Y. Yue, and Y. Song, "Finite-time cooperative-tracking control for networked Euler–Lagrange systems," *IET Control Theory Appl.*, vol. 7, no. 11, pp. 1487–1497, Jul. 2013.

[35] J. Mei, W. Ren, J. Chen, and G. Ma, "Distributed adaptive coordination for multiple Lagrangian systems under a directed graph without using neighbors' velocity information," *Automatica*, vol. 49, no. 6, pp. 1723–1731, Jun. 2013.

[36] T. Haidegger *et al.*, "Simulation and control for telerobots in space medicine," *Acta Astronautica*, vol. 81, no. 1, pp. 390–402, Dec. 2012.

[37] S. Blažič, "On periodic control laws for mobile robots," *IEEE Trans. Ind. Electron.*, vol. 61, no. 7, pp. 3660–3670, Jul. 2014.

[38] J. Chen, M. Gan, J. Huang, L. Dou, and H. Fang, "Formation control of multiple Euler–Lagrange systems via null-space-based behavioral control," *Sci. China Inf. Sci.*, vol. 59, no. 1, pp. 1–11, Jan. 2016.

[39] D. Li, W. Zhang, W. He, C. Li, and S. S. Ge, "Two-layer distributed formation-containment control of multiple Euler–Lagrange systems by output feedback," *IEEE Trans. Cybern.*, vol. 49, no. 2, pp. 675–687, Feb. 2019.

[40] H. Cai and J. Huang, "The leader-following consensus for multiple uncertain Euler–Lagrange systems with an adaptive distributed observer," *IEEE Trans. Autom. Control*, vol. 61, no. 10, pp. 3152–3157, Oct. 2016.

[41] M. Lu and L. Liu, "Leader-following consensus of multiple uncertain Euler–Lagrange systems subject to communication delays and switching networks," *IEEE Trans. Autom. Control*, vol. 63, no. 8, pp. 2604–2611, Aug. 2018.

[42] H.-X. Hu, G. Wen, W. Yu, Q. Xuan, and G. Chen, "Swarming behavior of multiple Euler–Lagrange systems with cooperation-competition interactions: An auxiliary system approach," *IEEE Trans. Neural Netw. Learn. Syst.*, vol. 29, no. 11, pp. 5726–5737, Nov. 2018.

[43] Y. Sun, L. Chen, G. Ma, and C. Li, "Adaptive neural network tracking control for multiple uncertain Euler–Lagrange systems with communication delays," *J. Frankl. Inst.*, vol. 354, no. 7, pp. 2677–2698, May 2017.

[44] L. Wang, M. F. Ge, Z. Zeng, and J. Hu, "Finite-time robust consensus of nonlinear disturbed multiagent systems via two-layer event-triggered control," *Inf. Sci.*, vol. 466, pp. 270–283, Oct. 2018.

[45] L. A. Montestruque and P. J. Antsaklis, "On the model-based control of networked systems," *Automatica*, vol. 39, no. 10, pp. 1837–1843, Oct. 2003.

[46] M. Fliess and C. Join, "Model-free control," *Int. J. Control*, vol. 86, no. 12, pp. 2228–2252, Jul. 2013.

[47] S. Vrkalovic, E.-C. Lunca, and I.-D. Borlea, "Model-free sliding mode and fuzzy controllers for reverse osmosis desalination plants," *Int. J. Artif. Intell.*, vol. 16, no. 2, pp. 208–222, 2018.

[48] D. Sun, X. Shao, and G. Feng, "A model-free cross-coupled control for position synchronization of multi-axis motions: Theory and experiments," *IEEE Trans. Control Syst. Technol.*, vol. 15, no. 2, pp. 306–314, Mar. 2007.

[49] M.-F. Ge, Z.-H. Guan, C. Yang, T. Li, and Y.-W. Wang, "Time-varying formation tracking of multiple manipulators via distributed finite-time control," *Neurocomputing*, vol. 202, pp. 20–26, Aug. 2016.

[50] M.-F. Ge, Z.-H. Guan, B. Hu, D.-X. He, and R.-Q. Liao, "Distributed controller–estimator for target tracking of networked robotic systems under sampled interaction," *Automatica*, vol. 69, pp. 410–417, Jul. 2016.

[51] Y. Su, P. C. Muller, and C. Zheng, "Global asymptotic saturated PID control for robot manipulators," *IEEE Trans. Control Syst. Technol.*, vol. 18, no. 6, pp. 1280–1288, Nov. 2010.

[52] J. Alvarez-Ramirez, R. Kelly, and I. Cervantes, "Semiglobal stability of saturated linear PID control for robot manipulators," *Automatica*, vol. 39, no. 6, pp. 989–995, Jun. 2003.

[53] H. Su, M. Z. Q. Chen, J. Lam, and Z. Lin, "Semi-global leader-following consensus of linear multi-agent systems with input saturation via low gain feedback," *IEEE Trans. Circuits Syst. I, Reg. Papers*, vol. 60, no. 7, pp. 1881–1889, Jul. 2013.

[54] J. Lyu, J. Qin, D. Gao, and Q. Liu, "Consensus for constrained multi-agent systems with input saturation," *Int. J. Robust Nonlinear Control*, vol. 26, no. 14, pp. 2977–2993, Dec. 2016.

[55] X. Wang, H. Su, X. Wang, and G. Chen, "Fully distributed event-triggered semiglobal consensus of multi-agent systems with input saturation," *IEEE Trans. Ind. Electron.*, vol. 64, no. 6, pp. 5055–5064, Jun. 2017.

[56] G. Cui, S. Xu, F. L. Lewis, B. Zhang, and Q. Ma, "Distributed consensus tracking for non-linear multi-agent systems with input saturation: A command filtered backstepping approach," *IET Control Theory Appl.*, vol. 10, no. 5, pp. 509–516, Mar. 2016.

[57] Z. Meng, Z. Zhao, and Z. Lin, "On global leader-following consensus of identical linear dynamic systems subject to actuator saturation," *Syst. Control Lett.*, vol. 62, no. 2, pp. 132–142, Feb. 2013.

[58] M. W. Spong, S. Hutchinson, and M. Vidyasagar, *Robot Modeling and Control*. Hoboken, NJ, USA: Wiley, 2006.

[59] G. Hardy, J. Littlewood, and G. Polya, *Inequalities*. Cambridge, U.K.: Cambridge Univ. Press, 1988.

[60] L. Wang, Z. Zeng, J. Hu, and X. Wang, "Controller design for global fixed-time synchronization of delayed neural networks with discontinuous activations," *Neural Netw.*, vol. 87, pp. 122–131, Mar. 2017.

[61] A. F. Filippov, *Differential Equations With Discontinuous Right-Hand Sides*. Dordrecht, The Netherlands: Kluwer, 1988.

[62] N. Fischer, R. Kamalapurkar, and W. E. Dixon, "LaSalle–Yoshizawa corollaries for nonsmooth systems," *IEEE Trans. Autom. Control*, vol. 58, no. 9, pp. 2333–2338, Sep. 2013.

Leimin Wang (M'18) received the B.S. degree in mathematics and applied mathematics from the South Central University for Nationalities, Wuhan, China, in 2011, and the Ph.D. degree in control science and engineering from the Huazhong University of Science and Technology, Wuhan, in 2016.

He is currently an Associate Professor with the School of Automation, China University of Geosciences, Wuhan. His current research interests include multiagent networks, neural networks, and memristors.

Haibo He (SM'11–F'18) received the B.S. and M.S. degrees in electrical engineering from the Huazhong University of Science and Technology, Wuhan, China, in 1999 and 2002, respectively, and the Ph.D. degree in electrical engineering from Ohio University, Athens, OH, USA, in 2006.

He is currently the Robert Haas Endowed Chair Professor with the Department of Electrical, Computer, and Biomedical Engineering, University of Rhode Island, Kingstown, RI, USA. He has published one sole-author research book (Wiley), edited one book (Wiley–IEEE) and six conference proceedings (Springer), and authored and coauthored over 300 peer-reviewed journals and conference papers. His current research interests include computational intelligence, machine learning, data mining, and various applications.

Dr. He was a recipient of the IEEE International Conference on Communications Best Paper Award in 2014, the IEEE CIS Outstanding Early Career Award in 2014, and the National Science Foundation CAREER Award in 2011. He is currently the Editor-in-Chief of the IEEE TRANSACTIONS ON NEURAL NETWORKS AND LEARNING SYSTEMS. He was the General Chair of the IEEE Symposium Series on Computational Intelligence in 2014.

Zhigang Zeng (SM'07) received the Ph.D. degree in systems analysis and integration from the Huazhong University of Science and Technology, Wuhan, China, in 2003.

He is currently a Professor with the School of Artificial Intelligence and Automation, Huazhong University of Science and Technology, where he is also with the Key Laboratory of Image Processing and Intelligent Control of the Education Ministry of China. He has published over 100 international journal papers. His current research interests include the theory of functional differential equations and differential equations with discontinuous right-hand sides, and their applications to dynamics of neural networks, memristive systems, and control systems.

Prof. Zeng was an Associate Editor of the IEEE TRANSACTIONS ON NEURAL NETWORKS from 2010 to 2011, and has been an Associate Editor of the IEEE TRANSACTIONS ON CYBERNETICS since 2014, the IEEE TRANSACTIONS ON FUZZY SYSTEMS since 2016, and an Editorial Board Member of *Neural Networks* since 2012, *Cognitive Computation* since 2010, and *Applied Soft Computing* since 2013.

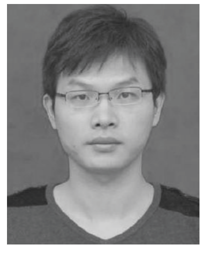

Ming-Feng Ge (M'17) received the B.Eng. degree in automation and the Ph.D. degree in control theory and control engineering from the Huazhong University of Science and Technology, Wuhan, China, in 2008 and 2016, respectively.

He is currently an Associate Professor with the School of Mechanical Engineering and Electronic Information, China University of Geosciences, Wuhan. His current research interests include networked robotic systems, formation tracking, and multiagent networks.

Authorized licensed use limited to: IEEE Editors-in-Chief. Downloaded on June 14,2021 at 19:52:24 UTC from IEEE Xplore. Restrictions apply.